Building and Environment 44 (2009) 1074–1080

Contents lists available at ScienceDirect

Building and Environment

journal homepage: www.elsevier.com/locate/buildenv

Simple method for determining daylight illuminance in a heavily obstructed environment

Danny H.W. Li*, Gary H.W. Cheung, K.L. Cheung, Joseph C. Lam

Building Energy Research Group, Department of Building and Construction, City University of Hong Kong, Tat Chee Avenue, Kowloon, Hong Kong, China

ARTICLE INFO

Article history:
Received 11 April 2008
Received in revised form 21 July 2008
Accepted 21 July 2008

Keywords:
Vertical daylight factor
Obstructions
Simulation
Ground reflection

ABSTRACT

Daylighting has long been recognized as an important issue in architecture. In Hong Kong many buildings are constructed close to each other and hence the external environment plays a significant role in building designs. Recently, vertical daylight factor (VDF) has been used as a criterion to justify the provision of natural lighting in buildings. This paper studies the calculation approach of VDF in a heavily obstructed environment. The techniques for determining the sky component and the reflected daylight from surrounding buildings and ground surfaces are described. Calculation tools in the form of simple equations and diagrams through computer-simulation analysis were established. The performance of the proposed method was evaluated against the daylight illuminance obtained by other independent computer simulations. It was found that predictions from the proposed approach were in good agreements with those produced by simulated results. The findings provide architects and building designers with a simple method for estimating the daylight illuminance at early design and planning stage.

1. Introduction

Being one of the most densely populated cities in the world, Hong Kong has faced many challenges in tackling housing needs. A large number of urban and suburban building projects have been developed to meet the ever-increasing demand. Most of the building developments are located in densely-built zones. To maximize the space from the limited land areas, apartment blocks of 40 storeys or more with eight to ten units on each floor are not uncommon. The shading effects due to surrounding buildings could substantially restrict the quantity of daylight penetrating into the building interior particularly for rooms at the lower floors [1,2]. In Hong Kong, the natural lighting design for building is governed by Part IV – Lighting and Ventilation, of the Building (Planning) Regulations CAP.123 (Laws of Hong Kong Chapter 123) [3]. Basically, the regulations prescribe two requirements for natural lighting. Internally, the required window area should not be less than one-tenth of the usable floor area. Externally, the separation between building blocks in the form of rectangular horizontal plan (RHP) in front of the window is governed by a vertical obstruction angle (α_B) which should not be more than 71.5° for habitable rooms and 76° for kitchens. The regulations have been in use for over 40 years and were demonstrated ineffective in contemporary Hong Kong [4].

In 2003, the Hong Kong Government issued a practice note on lighting and ventilation requirements. Based on a performance-based approach, the note adopted the vertical daylight factor (VDF) to specify the daylighting performance of the building. The minimum VDFs required are 8% for habitable room and 4% for kitchen [5]. In Hong Kong, kitchens of residential units are often situated in a deep reveal with windows placed inside deep recesses from the main façade and windows of habitable rooms facing narrow long streets are not uncommon [6]. Long urban canyons are one of main Hong Kong skyline features and external obstructions can be estimated based on a horizontal band. Most useful light entering the glazing into building interior come from a cone of light 100° centred to the normal of the glazing. The amount of this reflected light is dependent on how well these surrounding surfaces are illuminated and the reflectance of these surfaces [5]. It means that most available daylight for windows of lower and middle floors of a building surrounded by high-rise buildings is primarily through reflected light from the opposite buildings with various reflectance values. The ground reflected component would be small and a low ground reflectance of 0.2 is always adopted. However, the determination of VDF can be quite complex when the building faces large external obstructions. Advances in computer technology have reduced the time needed for illuminance calculation [7]. However, many practicing architects and engineers consider a full-scale computer simulation too complicated, costly and time-consuming when a number of building options and design schemes are being considered and evaluated. Moreover, not all architectural and engineering practices, who work on building

* Corresponding author. Tel.: +852 27887063; fax: +852 27887612.
E-mail address: bcdanny@cityu.edu.hk (D.H.W. Li).

0360-1323/$ – see front matter © 2008 Elsevier Ltd. All rights reserved.
doi:10.1016/j.buildenv.2008.07.011

projects, are familiar with lighting simulation programs [8]. The complex and sophisticated daylight software available is best used by an expert or experienced user [9]. Tregenza [10] modified the split-flux formulae and the method developed is an appropriate tool to estimate the VDF for windows facing large external obstructions. However, important parameters such as the fraction of flux reflected within the system (m_r) and the ratio of the direct skylight received by the ground to the horizontal illuminance of an unobstructed sky (E_g/E_h) were not further quantified. Also, the reflected light from ground (E_{rg}) may include certain amount of reflected light due to buildings below the horizon to the vertical window surface. Such issues may induce uncertainties and errors when the design tool is used. Previously, we developed simplified methods to compute daylight illuminance for rooms facing unobstructed standard skies [11–13]. This paper presents a calculation procedure to compute the VDF on facades facing large external obstructions. Design tools that include simple regression equations and diagrams are developed and evaluated against simulated results based on a lighting computer package and the Tregenza model. Characteristics of the findings and implications for daylighting designs are discussed.

2. Vertical daylight factor

Vertical daylight factor (VDF) is defined as the ratio in percentage of the total amount of daylight illuminance falling onto a vertical surface of a building to the instantaneous horizontal illuminance from a complete hemisphere of sky excluding direct sunlight. It takes into account light coming directly from the sky and reflected daylight from surrounding buildings and ground both above and below the horizon [5]. Mathematically, the VDF can be written as:

$$\mathrm{VDF} = \left(\frac{E_s + E_{rb} + E_{rg}}{E_h}\right) \times 100\% \quad (1)$$

where E_s = the light coming directly from the sky (lux); E_{rb} = the reflected light from obstructing buildings (lux); E_{rg} = the reflected light from ground (lux); E_h = the horizontal illuminance of an unobstructed sky (lux).

The illuminance on a plane, δE, resulting from a small patch of sky or obstruction is given by:

$$\delta E = L \cos\sigma \delta\omega \quad (2)$$

where L = the luminance of external elements (cd/m^2); ω = the solid angle (sr); σ = the angle between the sky elements or obstructions and the line normal to the plane (degrees).

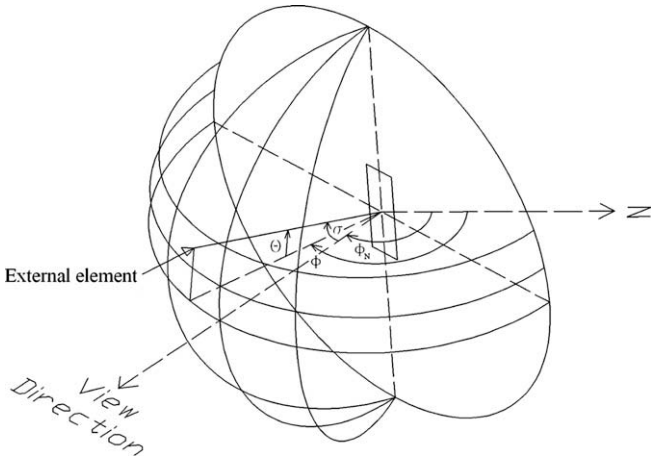

Fig. 1. Definition of angles for E determination.

Fig. 1 shows the definition of angles for E determination. The $\delta\omega$ and $\cos\sigma$ can be given as:

$$\delta\omega = \cos\theta\delta\theta\delta\phi \quad (3)$$

$$\cos\sigma = \cos\theta\cos(\phi - \phi_N) \quad (4)$$

where ϕ_N = the azimuth angle of the vertical surface normal (degrees).

The daylight illuminance received is mainly influenced by the luminance levels and patterns of the external elements (e.g. sky, obstructing buildings and ground surfaces) in the direction of views of the reference plane. An appropriate approach for determining the illuminance on a plane is to integrate the luminance distribution of the external element 'seen' by the plane. If the sky patches and the external obstructing surfaces were divided into n angular zones, then for numerical computation, the total amount of illuminance falling on the window façade E can be written as [14]:

$$E = \sum_i^n L_{\theta\phi i}\cos^2\theta_i \cos(\phi - \phi_N)_i \delta\theta_i \delta\phi_i \quad (5)$$

Using the numerical method means that the sky and obstructions must be subdivided into finite zones. The increasing of sky vault and obstruction divisions would lead to a more precise value of illuminance determination, but it requires longer computation time [15]. It is recommended that the celestial hemisphere split into 145 angular patches in bands of constant elevation in a 3-way symmetry about the zenith would be the appropriate subdivision [16], with sky scanner measurements based on this distribution [17]. Table 1 lists the altitude of band, azimuth increment and solid angle of individual sky zones under this subdivision of sky illuminance [18]. By counting the number of sky zones 'seen' by the reference vertical plane according to this pattern, E_s can be computed [11,12]. The counting approach is based on more than 50% of the sky zone viewable to the sensor. It should be pointed out that the method may be reasonable for simple skyline geometries such as infinitely-long urban canyons, but for complex environments, this could lead to calculation errors. Sky luminance data are essential to compute daylight illuminance but luminance distributions for the whole sky vault are far from being widely available. In 2003, the CIE adopted 15 standard skies [19] which cover the whole probable spectrum of skies found in nature. The distributions are described by continuous mathematical expressions that change smoothly in luminance from the horizon to zenith and with the angular distance from the sun. The luminance values of the 145 sky patches can be determined according to the particular sky standard. For reflected components, it is assumed that obstructing buildings and ground surfaces are perfectly diffusing and can be given as:

$$L_{rbi} = \frac{E_{rbi}\rho_b}{\pi} \quad (6)$$

where ρ_b = the reflectance of the obstructing buildings; E_{rbi} = the illuminance due to a small perfectly diffusing surface (i) of the external obstruction (lux); L_{rbi} = the reflected luminance due to a small perfectly diffusing surface (i) of the external obstruction (cd/m^2).

The first reflection of skylight from obstructing buildings onto the window façade (E_{rb1}) can be expressed as:

$$E_{rb1} = \sum_i^n L_{rbi}\omega_i\cos\sigma_i = \frac{\rho_b}{\pi}\sum_i^n E_{rbi}\omega_i\cos\sigma_i \quad (7)$$

The same subdivision approach for celestial hemisphere (Table 1) can be adopted for calculating E_{rb1}. Under obstructed environments,

Table 1
Subdivision of the sky (145 sky zones)

Altitude of band centre (°)	Number of zones in band	Azimuth increment (°)	Solid angle subtended by zone,[a] ω (sr)
6	30	12	0.0435
18	30	12	0.0416
30	24	15	0.0474
42	24	15	0.0407
54	18	20	0.0429
66	12	30	0.0445
78	6	60	0.0455
90	1	360	0.0344

[a] Solid angle $= 2\pi(\sin\gamma_u - \sin\gamma_l)$/number of zones in bands, where γ_u and γ_l are the upper and lower limits of the altitude band.

reflected light comes from below the horizon on the vertical window containing illuminance due to ground and lower parts of surrounding buildings which depends on the sine function of the angle between the reference vertical plane and the ground level of the opposite building ($\sin\alpha_L$). To compute the first reflection of skylight from ground onto the window façade (E_{rg1}), the reflected light from lower parts of surrounding buildings should be excluded. If the ground surfaces are assumed to be of perfectly diffusing, the E_{rg1}/E_h for an infinite-length urban canyon (as presented in Fig. 2) can be given as [20]:

$$\frac{E_{rg1}}{E_h} = \frac{\rho_g E_g(1-\sin\alpha_L)}{2E_h} \tag{8}$$

Once the E_g/E_h has been determined, the E_{rg1}/E_h can be obtained in accordance with Eq. (8). With a low mean value for ρ_g, it is not worthwhile to compute E_g/E_h to a high accuracy. Previously, values of 0.5 and 0.2 were adopted [10,21].

Inter-reflections appear between the external building surfaces and between buildings and the ground when the reference vertical plane facing large external obstruction [10]. This is a second-order effect and an estimate of its magnitude is sufficient. The total flux on the window from reflected daylight originally incident on obstructing buildings and ground is approximately [22]:

$$\begin{aligned} E_{rb} + E_{rg} &= (E_{rb1} + E_{rg1})\left(1 + \rho_o + \rho_o^2 + \rho_o^3 + \cdots\right) \\ &= (E_{rb1} + E_{rg1})\left(\frac{1}{1-\rho_o}\right) \end{aligned} \tag{9}$$

where ρ_o = the effective mean external reflectance.

The ρ_o depends on the effective areas and reflectance values of the obstruction surfaces and the ground, and the fraction of flux reflected within the system (m_r). By taking the effective areas of building façade and ground are approximately the same, ρ_o can be written as [10]:

$$\rho_o = m_r\frac{\rho_b + \rho_g}{2} \tag{10}$$

Tregenza [10] assumed $m_r = 0.5$ and Ng [21] adopted $m_r = 0.7$ for conditions of high obstruction.

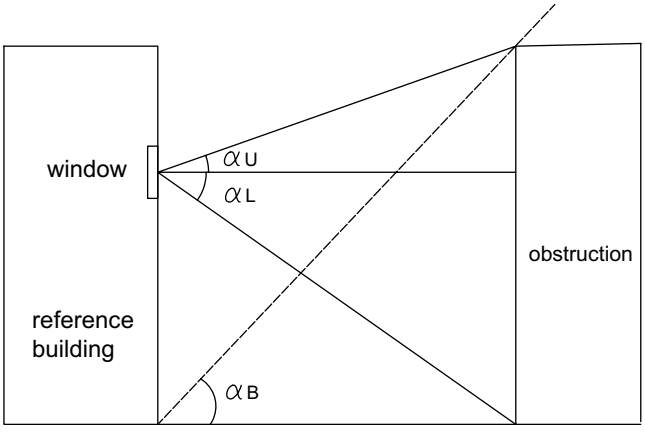

Fig. 2. The angles between the façade of the reference building and the obstructing building.

3. Computer-simulation approach

The success of a daylighting scheme depends very much on a good understanding of the subtle interactions of a large number of design features. It is generally accepted that a detailed lighting simulation program is an appropriate design tool to determine and evaluate the impact of related factors, particularly for performance-based approaches. Simple design methods in the form of simple equations, charts and tables through comprehensive computer-simulation studies are useful during the initial-design stage, when different design schemes and concepts are being considered and assessed. It is envisaged that such correlation relationships and simple design tools can give architects and engineers certain basic and concise insights into the interdependency among various design parameters. Building professions do make computer simulations after the design schemes have been finalized for submission and presentation.

Owing to the advancements of computer technology, there has been a steady increase in the use of computer-simulation techniques to evaluate daylighting performance. The simulation tool employed in the present study is a lighting simulation program called RADIANCE which has been used by a number of researchers to compute interior illuminances [23–26]. It is a computer-simulation package for simulating and visualizing lighting in and around architectural environments. It has been reported that RADIANCE lighting simulation system could predict internal illuminance to high degree of accuracy for a range of realistic sky conditions [27,28]. It can examine advanced lighting regimes using the backward ray-tracing technique, in which light is traced from the observer to the dominant light sources to calculate the luminances required for visualization. RADIANCE is available in several versions. In the present study, the analysis was based on the RADIANCE version 3.8 developed at Lawrence Berkeley Laboratory running under UNIX workstation.

4. Design tools development and evaluation

External obstructions influence the daylighting performance in two aspects. First is the amount of sky being obstructed or unobstructed. Second is the reflectance of obstructing buildings and the ground reflected component. The former depends on the height and length of neighboring buildings and the separations. When buildings are located close to each other, shading effect can be severe, particularly for the units at the lower floors. For the sake of convenience, the effect of external obstruction can be represented by angle of obstruction. The latter, in practice, is to assume average reflectance values for surrounding buildings and ground. The illuminance on the window of a high-rise building facing severe sky obstruction was simulated to develop the design tools. Since most useful light entering building interiors come from the sky normal to the glazing façade, it was assumed that the obstructing block was located in front of the reference building. An infinite-length urban canyon as presented in Fig. 2 was adopted. This urban skyline feature was used to examine the urban wind and daylight environments by a number of researchers [29–32]. The upper obstructing angle (α_U) and lower obstructing angle (α_L) represent

the shading effect with respect to the reference point of the vertical plane and $\tan\alpha_B = \tan\alpha_U + \tan\alpha_L$. A series of computer simulations were carried out with the obstructing angles and reflectance of external elements being changed parametrically. The α_U and α_L were varied ranging from 10° to 70° and ρ_b was altered between 0.2 and 0.6. The typical ρ_g of 0.2 [21,33,34] and the traditional CIE overcast sky condition (i.e. CIE sky standard 1) were employed for approach development.

Totally, three important parameters namely, E_{rb1}, ρ_o, E_g/E_h, were analyzed through the thorough simulations to obtain reliable values for VDF determination. As indicated in Eq. (7), E_{rb1} strongly depends on E_{rbi} which varies with the height of the obstructions. To simplify the calculation, an average value of daylight illuminance received by the obstructing building (E_{aveS}) should be adopted. It is expected that E_{aveS} can be predicted based on the daylight illuminance at the top of the obstructions (E_{topS}) which can be obtained by numerical method [11–13]. The ratio of E_{aveS} to E_{topS} was plotted against α_U at various α_L and Fig. 3 exhibits the results. At small obstructing angles, for instance α_U and $\alpha_L = 10°$, the E_{aveS}/E_{topS} is around 0.88. When $\alpha_U = 70°$ and $\alpha_L = 10°$, E_{aveS}/E_{topS} reduces to around 0.19. With α_U close to 80°, E_{aveS}/E_{topS} tends to almost zero. Through regression analysis, a quadratic function was formed and is given as:

$$\frac{E_{aveS}}{E_{topS}} = \left(0.92 - 2.7\times10^{-3}\alpha_U - 1.1\times10^{-4}\alpha_U^2\right)\times 0.935^{\left(\frac{\alpha_L}{10}-1\right)} \quad \left(R^2 = 0.999\right) \tag{11}$$

As the R^2 is close to unity, the equation is perfectly correlated and E_{aveS} can be accurately computed. Substituting E_{aveS} for E_{rbi} in Eq. (7) the E_{rb1} can be calculated. To determine the E_{rg1}, the E_g/E_h at different obstructed conditions should be determined. In a heavily obstructed environment, ground reflected component can be significant. Fig. 4 displays the correlation between E_g/E_h and α_B. Without sky obstruction and completely obstructed, E_g/E_h should be equal to 1 and 0, respectively. As the α_B increases, the E_g/E_h decreases gently. The E_g/E_h is around 0.5 at α_B of 45°. When $\alpha_B = 80°$, E_g/E_h drops to just more than 0.1. A linear regression analysis is carried out and E_g/E_h can be expressed in terms of α_B as follows:

$$\frac{E_g}{E_h} = 1 - 0.011\alpha_B \tag{12}$$

The R^2 is more than 0.98, indicating that over 98% of the changes in E_g/E_h can be explained by the variations in α_B. As shown in the figure, E_g/E_h is perfectly fitted when α_B is larger than 40°. Under

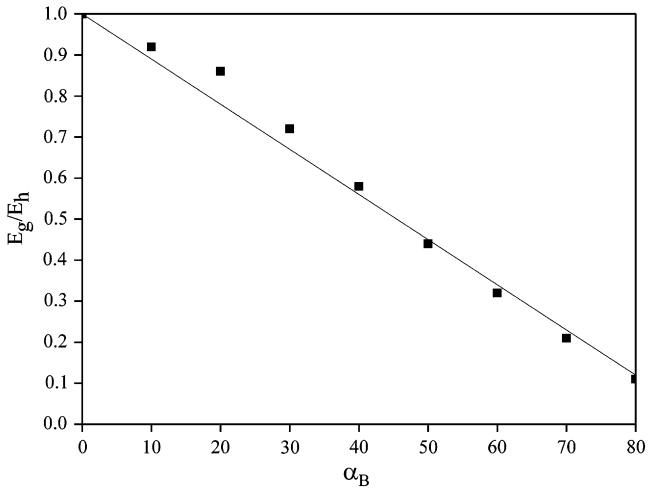

Fig. 4. Correlation between E_g/E_h and α_B.

heavily obstructed conditions, only small amount of sky patches contribute E_g and the variations would be quite small for different overcast sky patterns. It shows that E_g/E_h can be accurately estimated in highly obstructed environments. The ρ_o is the key parameter to calculate the external reflected components. It would be appropriate to find out the ρ_o at various α_L, α_U and ρ_b according to the simulated results. Fig. 5 shows the plot between ρ_o and α_U at various α_L with $\rho_b = 0.2$. It can be seen that ρ_o increases with increasing α_U and α_L. When α_L is 40° or more, ρ_o varies slightly. Very similar pattern can be observed for other ρ_b. As shown in Eq. (10), with large ρ_b values, higher ρ_o levels are resulted. Regression analysis has suggested that ρ_o can be expressed as a function of α_U and ρ_b at different α_L as:

$$\rho_o = \left(0.0391 + 0.00219\alpha_U - 6.049\times10^{-6}\alpha_U^2\right)(4.213\rho_b + 0.157) \text{ for } \alpha_L = 10° \tag{13}$$

$$\rho_o = \left(0.0681 + 0.00159\alpha_U - 1.022\times10^{-6}\alpha_U^2\right)(4.213\rho_b + 0.157) \text{ for } \alpha_L = 20° \tag{14}$$

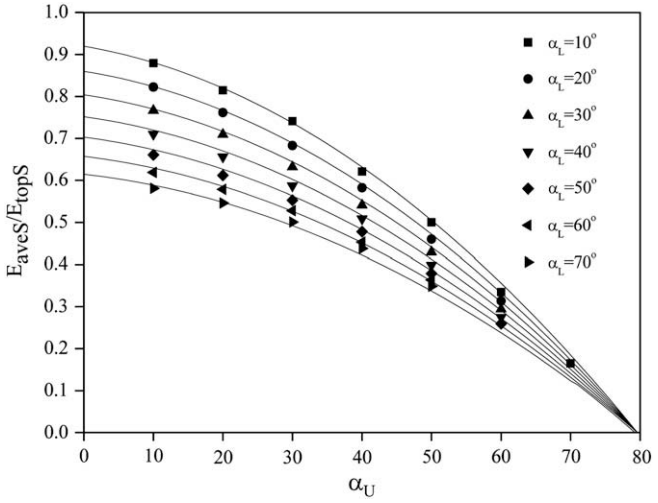

Fig. 3. Correlation between the E_{aveS}/E_{topS} and α_U at various α_L.

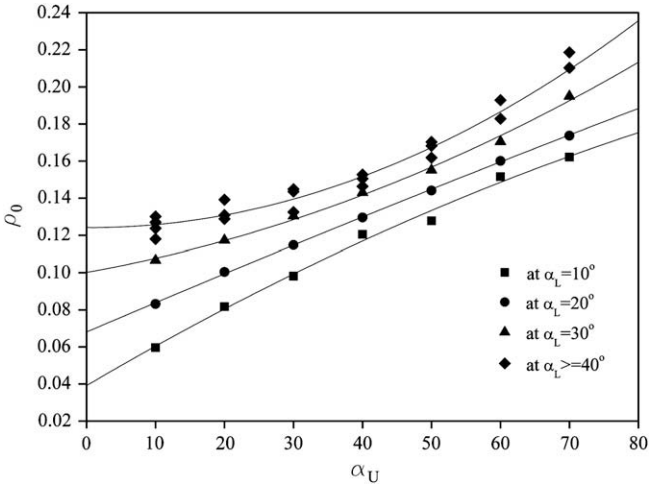

Fig. 5. Correlation between ρ_o and α_U at various α_L with $\rho_b = 0.2$.

Table 2
The E_s, E_{rb} and E_{rg} obtained using the proposed method

Upper obstructing angle, α_U (°)	Lower obstructing angle, α_L (°)	Sky component, E_s (%)	Obstruction reflected component, E_{rb} (%)	Ground reflected component, E_{rg} (%)
60	10	7.52	3.90	3.58
60	20	7.52	4.36	2.71
60	30	7.52	4.78	1.97
60	40	7.52	5.12	1.33
60	50	7.52	5.18	0.78
70	10	3.44	2.13	2.57

$$\rho_o = \left(0.1 + 6.59 \times 10^{-4}\alpha_U + 9.43 \times 10^{-6}\alpha_U^2\right)(4.213\rho_b + 0.157) \text{ for } \alpha_L = 30^\circ \quad (15)$$

$$\rho_o = \left(0.124 - 1.9 \times 10^{-5}\alpha_U + 1.767 \times 10^{-5}\alpha_U^2\right)(4.213\rho_b + 0.157) \text{ for } \alpha_L \geq 40^\circ \quad (16)$$

All the R^2 values are more than 0.99, indicating very strong correlations for Eqs. (13)–(16) and accurate ρ_o can be determined accordingly. In summary, the steps to predict the VDF are outlined as follows:

- Determine the obstructing angles α_U and α_L and the angles to compute E_{topS}.
- Compute the E_s using the numerical equation (Eq. 5).
- Compute the E_{topS} using the numerical equation (Eq. 5).
- Obtain E_{aveS} using Eq. (11) or Fig. 3 according to the required α_U and α_L.
- Substitute E_{aveS} for E_{rbi} in Eq. (7) to calculate E_{rb1}.
- Compute E_{rg1} using Eq. (8) and E_g/E_h can be obtained from Eq. (12).
- Determine $E_{rb} + E_{rg}$ using Eq. (9) and ρ_o can be obtained using Eqs. (13)–(16) or Fig. 5.
- Sum up E_s, E_{rb} and E_{rg} to obtain the VDF.

5. Worked examples and discussion

The application of this simple estimation method can best be illustrated with worked examples. This can give a feel for the errors induced by various approaches. The examples were based on an infinite length urban canyon with the $\rho_b = 0.4$ and $\rho_g = 0.2$. To consider heavily obstructed environments, $\alpha_U = 60^\circ$ at various α_L ranging from 10° to 50°, $\alpha_U = 70^\circ$ with $\alpha_L = 10^\circ$ were examined. Accordingly, the E_s, E_{rb} and E_{rg} were determined and Table 2 summarizes the findings. The E_s for $\alpha_U = 60^\circ$ and 70° are 7.52% and 3.44%, respectively. Under a heavily obstructed sky, more flux is interreflected and m_r becomes larger. At $\alpha_U = 60^\circ$, the E_{rb} increases from 3.9% with $\alpha_L = 10^\circ$ to 5.18% with $\alpha_L = 50^\circ$. As α_L increases, the effective area of ground becomes smaller. The E_{rg} is only 0.78% when $\alpha_U = 60^\circ$ and $\alpha_L = 50^\circ$. The results also indicate that the ground reflection can be significant in heavily obstructed environments such as rooms at lower floor level facing high-rise buildings (i.e. very large α_U and small α_L). For instance, at $\alpha_U = 70^\circ$ and $\alpha_L = 10^\circ$, E_{rb} can be less than E_{rg} which represents over a quarter of the VDF. For large α_L, E_{rg} is far less than E_{rb}.

A comparative study on VDF predicted by the RADIANCE simulation software, the proposed method and Tregenza's modified split-flux formulae were conducted. To further evaluate the ground reflectance, $\rho_g = 0.15$ was also considered. Table 3 presents the results. With $\alpha_U = 60^\circ$, the VDFs were simulated ranging from 14.76% at $\alpha_L = 10^\circ$ to 13.51% at $\alpha_L = 50^\circ$. When $\alpha_U = 70^\circ$ and $\alpha_L = 10^\circ$, the simulated VDF of 8.2% was found. Using the proposed approach, the VDFs were in very good agreement with those simulated data with the variation of less than 0.2% in most cases. With $\rho_g = 0.15$, the peak discrepancy would be of about 1.1% comparing with the results obtained by the proposed method using $\rho_g = 0.2$. It indicates that a value of 0.2 for ρ_g is a reasonable assumption in dense urban environments. When Tregenza's modified split-flux formulae were considered, VDF was independent of α_L for a particular α_U. With both m_r and $E_g/E_h = 0.5$, the VDFs were 9.29 and 6.36% for $\alpha_U = 60^\circ$ and 70°, respectively. When $m_r = 0.7$ and $E_g/E_h = 0.2$ were used, the VDF reduced to 6.35% for $\alpha_U = 60^\circ$ and decreased to 3.38% for $\alpha_U = 70^\circ$. The difference with respect to the simulated VDF can be more than 8.4%. There are three main causes contributing the discrepancy. Firstly, a fixed angular height was used for the double integrals in the Tregenza method. For fixed-height blocks parallel with the window wall, the angular height will drop from the centre of the reference window toward two ends. Using numerical approach, this drawback can be eliminated. Daylight graphs such as Waldram Diagram is a useful calculation procedure for E_s determination with reliable results [11,12,35]. Secondly, constant values for m_r and E_g/E_h were used. Under a dense urban environment, m_r and E_g/E_h can be important and change with various obstructed conditions. Accurate VDF may not be computed using fixed m_r and E_g/E_h values. Also, the light coming from below the horizon includes reflected light due to ground and buildings below the horizon to the vertical window. However, only ground reflected component of infinite long is considered. The VDF may be further underestimated when ρ_b is of a high value.

To assess whether the regression equations established are applicable to various obstructed conditions, the VDFs estimated by the regression models were compared with other independent results under CIE standard sky 1. Fig. 6 presents the plot of simulated and estimated VDF results using the proposed approach. A linear trend between the estimated and simulated data is evident. For large VDF values, sky component is the dominant factor (i.e. tends to an unobstructed sky) and the estimated results are just slightly less than those simulated data. At low VDF values (i.e. externally reflected component dominant), the predicted data are in very good agreement with the corresponding simulated values. To further examine the behavior of the modeled equations, analysis was extended to other overcast skies. In this connection, 4 other CIE

Table 3
Comparison of VDF obtained using various methods

Upper obstructing angle, α_U (°)	Lower obstructing angle, α_L (°)	Simulated by RADIANCE ($R_g = 0.2$) (%)	Proposed method ($R_g = 0.2$) (%)	Simulated by RADIANCE ($R_g = 0.15$) (%)	Tregenza's method with $m_r = 0.5$ and $E_g/E_h = 0.5$	Tregenza's method with $m_r = 0.7$ and $E_g/E_h = 0.2$
60	10	14.76	14.99	13.89	9.29	6.35
60	20	14.41	14.59	13.74	9.29	6.35
60	30	14.07	14.27	13.59	9.29	6.35
60	40	13.77	13.96	13.43	9.29	6.35
60	50	13.51	13.47	13.28	9.29	6.35
70	10	8.2	8.15	7.61	6.36	3.38

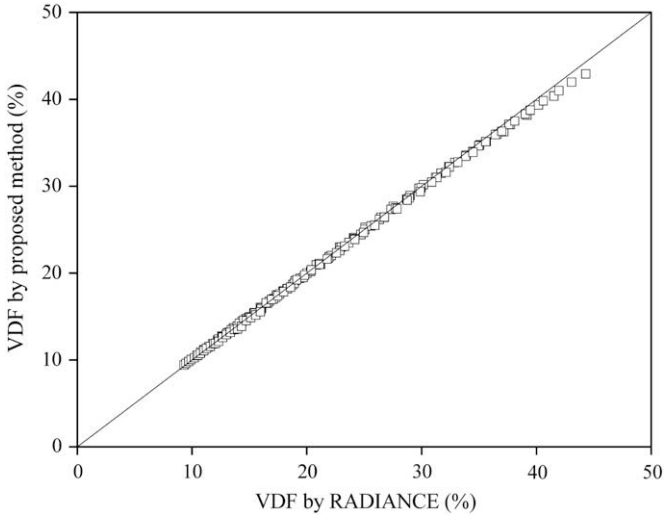

Fig. 6. Simulated and estimated VDFs for CIE sky 1.

overcast skies (i.e. CIE standard skies 2–5) were employed. Since sky standards 2 and 4 are slight brightening toward the sun, solar positions that in front of and behind the window façade at elevations of 30° and 60° were set for these two sky types. Again, the RADIANCE software was used to simulate the data and Fig. 7 shows the VDF results. Although the data are more scattered comparing with Fig. 6, a clustered band can be clearly identified. The closeness of the predicted values to the simulated results was further evaluated in terms of relative root mean square error (RRMSE):

$$\text{RRMSE} = \sqrt{\frac{\sum (e_i)^2}{N}} \tag{17}$$

$$e_i = \left[\frac{\text{VDF}_{\text{P}i} - \text{VDF}_{\text{S}i}}{\text{VDF}_{\text{S}i}}\right] \times 100\% \tag{18}$$

where $\text{VDF}_{\text{P}i}$ = the predicted VDF (%); $\text{VDF}_{\text{S}i}$ = the simulated VDF (%); N = number of data.

Table 4 summarizes the results under the five overcast skies (i.e. CIE standard skies 1–5). For CIE standard sky 1, the RRMSE was calculated to be 1.1% and the e_i ranging from −3.1% to 1.5%.

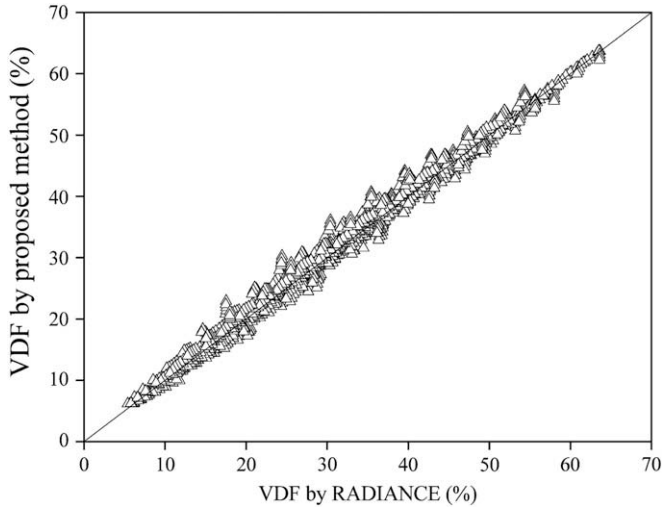

Fig. 7. Simulated and estimated VDFs for CIE skies 2 to 5.

Table 4
Summary of relative root mean square error (RRMSE) for vertical daylight factors (VDFs) under different CIE overcast skies

	RMSE (%)	e_i (highest) (%)	e_i (lowest) (%)
Sky standard 1	1.1	1.5	−3.1
Sky standard 2	4.2	16.4	−15.7
Sky standard 3	3.4	9.4	−0.2
Sky standard 4	6.2	30.7	−11.2
Sky standard 5	6.6	17.7	1.0

It is argued that the VDF can be perfectly modeled under this sky type. This is not surprising, given that the modeled equations were established under such a sky condition. For other overcast skies, the RRMSE varies between 3.4 and 6.6% and the e_i ranges from −15.7% for sky standard 2 to 30.7% for sky standard 4. A detailed examination of the results revealed that such peak discrepancies appear when the window façade is in front of (i.e. −15.7% for sky standard 2) and behind the sun (i.e. 30.7% for sky standard 4). Totally, 703 out of 740 cases (i.e. over 95% of all cases) were with the discrepancy values of less than 15% in sky standard 4. For sky standard 2, only 2 cases (i.e. less than 0.3% of all cases) were with discrepancy values of more than 15%. As the RRMSE is less than 6.6% for all five overcast sky conditions, the proposed modeled equations can be applicable and appropriate to places where overcast skies particularly the sky standards 1 and 3 occur more frequently [36–38].

6. Conclusions

A procedure involving computer-simulation techniques was employed to study the vertical daylight factor (VDF) under infinitely-long urban canyons with the ground reflectance of 0.2. Justifications of this skyline feature were made. Results from the simulation runs were used to establish a number of correlation equations for determining the key parameters. Different components under various heavily obstructed environments were elaborated and discussed. A comparative study on VDF predicted by the RADIANCE simulation software, the proposed method and Tregenza's modified split-flux formulae were conducted. It was found that the VDFs predicted based on the proposed approach were in good agreement with those simulated by the RADIANCE and a value of 0.2 for ρ_g is a reasonable assumption in dense urban environments. The results obtained using Tregenza's model were quite small and the peak VDF difference can be more than 8.4%. The main causes for the discrepancy were demonstrated. The performance of the proposed models was evaluated against independent simulated results using the RADIANCE software. It was found that the relative root mean square error (RRMSE) ranges from 1.1% for sky standard 1 to 6.6% for sky standard 5. In general, the modeled equations and RADIANCE software can give similar VDF values and the proposed approach can be applied to overcast sky conditions particularly the sky standards 1 and 3. Checking the accuracy of the proposed procedure will be carried out in the future when more reliable measured data in the form of scale model and building measurements under various real sky conditions are available. The work was based on the CIE standard skies that cover the whole probable spectrum of skies in the world. It is expected that the concept and procedures developed in this study can be used to other cities with similar high-rise urban developments. Although we only illustrate the approach for overcast sky conditions, the model could be applicable to non-overcast skies (i.e. dynamic conditions) with appropriate corrections and modifications. An annual inter model comparison of the proposed model against a dynamic simulation engine could constitute an intermediary validation solution.

Acknowledgements

The work described in this paper was fully supported by a Public Policy Research Exercise from the Research Grants Council of the Hong Kong Special Administrative Region, China (Project No. CityU 1001-PPR-2). G.H.W. Cheung was supported by a City University of Hong Kong studentship.

References

[1] Li DHW, Lo SM, Lam JC, Yuen RKK. Daylighting performance in residential buildings. Architectural Science Review 1999;42(3):213–9.
[2] Li DHW, Wong SL, Tsang CL, Cheung GHW. A study of the daylighting performance and energy use in heavily obstructed residential buildings via computer simulation techniques. Energy and Buildings 2006;38(11):1343–8.
[3] Hong Kong Government. Laws of Hong Kong chapter 123 building (planning) regulations – lighting and ventilation. Hong Kong; 1997.
[4] Ng E. Regulate for light, air and healthy living part 3 – the becoming of PNAP278. Hong Kong Institute of Architects Journal 2005;44(4):16–25.
[5] Buildings Department, HKSAR. Lighting and ventilation requirements – performance-based approach, practice note for authorized persons and registered structural engineers PNAP278. China: The Government of the Hong Kong Special Administrative Region; 2003.
[6] Ng E. Studies on daylight design and regulation of high residential housing in Hong Kong. Lighting Research and Technology 2003;35(2):127–39.
[7] Galasiu AD, Atif MR. Applicability of daylighting computer modelling in real case studies: comparison between measured and simulated daylight availability and lighting consumption. Building and Environment 2002;37(4):363–77.
[8] Betman E. Daylight calculations using constant luminance curves. Renewable Energy 2005;30(2):241–57.
[9] Jones PJ, Alexander D, Marsh A, Burnett J. Evaluation of methods for modelling daylight and sunlight in high rise Hong Kong residential buildings. Indoor and Built Environment 2004;13(4):249–58.
[10] Tregenza PR. Modification of the split-flux formulae for mean daylight factor and internal reflected component with large external obstructions. Lighting Research and Technology 1989;21(3):125–8.
[11] Li DHW, Lau CCS, Lam JC. A simplified procedure using daylight coefficient concept for sky component prediction. Architectural Science Review 2004;47(3):287–94.
[12] Li DHW, Cheung GHW, Lau CCS. A simplified procedure for determining indoor daylight illuminance using coefficient concept. Building and Environment 2006;41(5):578–89.
[13] Li DHW, Cheung GHW. Average daylight factor for the 15 CIE standard skies. Lighting Research and Technology 2006;38(2):137–52.
[14] Li DHW, Lau CCS, Lam JC. Predicting daylight illuminance on inclined surfaces using sky luminance data. Energy 2005;30(9):1649–65.
[15] Cesarano A, Bellia A, Minichiello L, Sibilio S. Sky luminance models: sensitivity to sky-dome subdivision. Lighting Research and Technology 1996;28(3):131–40.
[16] Tregenza PR. The sensitivity of room daylight to sky brightness. Architectural Science Review 1999;42(2):129–32.
[17] CIE – Commission Internationale de l'Eclairage. Guide to recommended practice of daylight measurement. Sien, CIE; 1994.
[18] Tregenza PR, Sharples S. New daylight algorithm. University of Sheffield; 1995.
[19] CIE S 011/E. Spatial distribution of daylight-CIE standard general sky. Standard. Vienna: CIE Central Bureau; 2003.
[20] Tregenza PR. Mean daylight illuminance in rooms facing sunlit streets. Building and Environment 1995;30(1):83–9.
[21] Ng E. A simplified daylighting design tool for high-density urban residential buildings. Lighting Research and Technology 2001;33(4):259–72.
[22] Cheung HD, Chung TM. Calculation of the vertical daylight factor on window facades in a dense urban environment. Architectural Science Review 2005;48(1):81–92.
[23] Reinhart CF, Herkel S. The simulation of annual daylight illuminance distributions-a state-of-the-art comparison of six RADIANCE-based methods. Energy and Buildings 2000;32(2):167–87.
[24] Ng EYY, Lam KP, Wu W, Nagakura T. Advanced lighting simulation in architectural design in tropics. Automation in Construction 2001;10(3):365–79.
[25] Li DHW, Lau CCS, Lam JC. Predicting daylight illuminance by computer simulation techniques. Lighting Research and Technology 2004;36(2):113–29.
[26] Chung TM, Cheung HD. Assessing daylighting performance of buildings using orthographically projected area of obstructions. Journal of Light and Visual Environment 2006;30(2):28–34.
[27] Mardaljevic J. Validation of a lighting simulation program under real sky conditions. Lighting Research and Technology 1995;27(4):181–8.
[28] Gugliermetti F, Grignaffini S, Bisegna F. Computer simulations, full and scale model measurements as design tools to assess daylight factors in underground open space, Proceedings of Istanbul 2001 – international lighting congress. Istanbul, Turkey: Istanbul Technical University; 12–14 September 2001. p. 519–26.
[29] Oke TR. Street design and urban canopy layer climate. Energy and Buildings 1998;11(2):103–13.
[30] Tsangrassoulis A, Santamouris M, Geros V, Wilson M, Asimakopoulos D. A method to investigate the potential of south-oriented vertical surfaces for reflecting daylight onto oppositely facing vertical surfaces under sunny conditions. Solar Energy 1999;66(6):439–46.
[31] Tsangrassoulis A, Santamouris M. Numerical estimation of street canyon albedo consisting of vertical coated glazed façades. Energy and Buildings 2003;35(5):527–31.
[32] Chaiyakul Y. Estimating daylight in urban streets in Bangkok. Architectural Science Review 2004;47(2):121–30.
[33] CIBSE. CIBSE guide A2. London: Chartered Institution of Building Services Engineers; 1982.
[34] Serra R. Chapter 6 – daylighting. Renewable and Sustainable Energy Reviews 1998;2(1–2):115–55.
[35] Hopkinson RG, Petherbridge P, Longmore J. Daylighting. London, UK: Heinemann; 1966.
[36] Tregenza PR. Standard skies for maritime climates. Lighting Research and Technology 1999;31(3):97–106.
[37] Enarun D, Littlefair PJ. Luminance models for overcast skies: assessment using measured data. Lighting Research and Technology 1995;27(1):53–8.
[38] Li DHW, Lau CCS, Lam JC. Standard skies classification using common climatic parameters. Journal of Solar Energy Engineering 2004;126(3):957–64.